Peer-reviewed version available at *Molecules* **2019**, *24*, 3615; doi:10.3390/molecules24193615

Article

The Power of LC-MS Based Multiomics: Exploring Adipogenic Differentiation of Human Mesenchymal Stem/Stromal Cells

Evelyn Rampler[1]*, Dominik Egger[2], Harald Schoeny[1], Mate Rusz[1], Maria Pires Pacheco[3], Giada Marino[3], Cornelia Kasper[2], Thomas Naegele[3] and Gunda Koellensperger[1]

[1] University of Vienna, Institute of Analytical Chemistry, Währinger Str. 38, 1090 Vienna, Austria; evelyn.rampler@univie.ac.at
[2] University of Natural Resources and Life Sciences, Muthgasse 18, 1190 Vienna, Austria; dominik.egger@boku.ac.at
[3] LMU München, Department Biology I, Großhaderner Str. 2-4, 82152 Planegg-Martinsried, Germany; thomas.Naegele@biologie.uni-muenchen.de

* Correspondence: evelyn.rampler@univie.ac.at

Abstract

The molecular study of fat cell development in the human body is essential for our understanding of obesity and related diseases. Mesenchymal stem/stromal cells (MSC) are the ideal source to study fat formation as they are the progenitors of adipocytes. In this work, we used human MSCs, received from surgery waste, and differentiate them into fat adipocytes. The combination of several layers of information coming from lipidomics, metabolomics and proteomics enabled network analysis of the biochemical pathways in adipogenesis. Simultaneous analysis of metabolites, lipids and proteins in cell culture is challenging due to the compound's chemical difference so that most studies involve separate analysis with unimolecular strategies. In this study, we employed a multimolecular approach using a two–phase extraction to monitor the crosstalk between lipid metabolism and protein-based signaling in a single sample (~10^5 cells). We developed an innovative analytical workflow including standardization with in-house produced ^{13}C-isotopically labeled compounds, hyphenated high-end mass spectrometry (high-resolution Orbitrap MS) and chromatography (HILIC, RP) for simultaneous untargeted screening and targeted quantification. Metabolite and lipid concentrations ranged over 3-4 orders of magnitude and were detected down to the low fmol (absolute on column) level. Biological validation and data interpretation of the multiomics workflow was performed based on proteomics network reconstruction, metabolic modelling (MetaboAnalyst 4.0) and pathway analysis (OmicsNet). Comparing MSCs and adipocytes, we observed significant regulation of different metabolites and lipids such as triglycerides, gangliosides and carnitine with 113 fully reprogrammed pathways. The observed changes are in accordance with literature findings dealing with adipogenic differentiation of MSC. These results are a proof of principle for the power of multimolecular extraction combined with orthogonal LC-MS assays and network construction. Considering the analytical and biological validation performed in this study, we conclude that the proposed multiomics workflow is ideally suited for comprehensive follow-up studies on adipogenesis and is fit for purpose for different applications.

Keywords: LC-MS; mesenchymal stem cells; stromal cells; fat differentiation; lipidomics; metabolomics; proteomics; multiomics; network analysis; mathematical modelling

1. Introduction

In the context of obesity-related diseases it is essential to understand the molecular mechanisms that govern the formation of fat cells from stem cells. Mesenchymal stem/stromal cells (MSCs) are multi-potent stem cells and the actual progenitors of fat cells/adipocytes[1]. MSCs are easily accessible as they can be derived from surgical waste or biopsies, i.e. bone marrow, birth-associated tissue and adipose tissue. Due to their high proliferation capacity, immune-modulatory functions and potential to differentiate into multiple lineages, MSC carry a huge clinical promise in cell-based therapies, immunomodulation and tissue engineering[2–5]. In contrast, induced pluripotent stem cells (iPSCs) are still not considered as safe since they are genetically not stable[6]. Also, MSCs are ethically not questionable like embryonic stem cells. Today adipose tissue is the predominant cell source for MSCs[2,7] as they can be obtained more easily and efficiently than from bone marrow[4]. The process of adipocyte formation, also known as adipogenesis, is regulated by a network of complex molecular processes. Adipocyte differentiation acts via signal transduction of hormones, growth factors, metabolites, lipids and specific protein receptors mediating external growth and differentiation signals through a cascade of intracellular events. In general, fat cell differentiation is triggered by the ceramide and peroxisomal proliferator-activated receptor gamma (PPARγ) [8–10]. Insulin and insulin-like growth factor 1 (IGF-1) are required for fat cell formation and activate distinct downstream signal transduction pathways such as (1) a phosphorylation-dephosphorylation mechanism subsequent to IGF-1 tyrosine phosphorylation or (2) insulin activation of the phosphatidylinositol 3-kinase pathway[11]. During the terminal differentiation phase, adipocytes *de novo* lipogenesis and insulin sensitivity is highly increased. Protein and mRNA levels for enzymes (e.g. stearoyl-CoA desaturase, glycerol-3-phosphate dehydrogenase, fatty acid synthase) involved in triacylglycerol metabolism are increased 10-100-fold upon fat cell formation[11].

In order to follow MSC differentiation into fat cells, suitable analytical workflows are necessary. Omics based strategies are ideal for adipocyte differentiation analysis as they are based on the observation of an entire subset of molecules in one organism. In this work, we appy a multiomics workflow combining metabolomics, lipidomics and proteomics. Mass spectrometry (MS) based multiomics strategies are extremely powerful due to their unrivaled potential to monitor an entire set of molecules in order to follow cellular metabolism and perturbations[12–14]. The combination of liquid chromatography (LC) with high-resolution MS is ideally suited for multimolecular chemical analysis as LC-MS enables identification and quantification by (1) retention time, (2) accurate mass and (3) fragmentation pattern of hundreds to thousands of compounds in parallel. Metabolomics of stem and fat cells provides information on the phenotypic change of small metabolites involved in the differentiation process. With lipid droplet formation as hallmark of adipogenic differentiation[11], lipidomics is able to reflect elevated lipid content at the same time providing information on MSCs and adipose tissue lipid pattern. Proteomics on the other hand, enables to monitor important protein key players involved into fat cell formation. In our workflow, we aim to merge targeted quantification and non-targeted screening of metabolites and lipids to follow MSC differentiation in adipocytes. The absolute accurate quantification of several hundreds of lipids remains a field of analytical development as desirable lipid compound-specific standardization is a challenge due to the complexity of the lipidome. Recently, we developed the novel Lipidome Isotope Labeling of Yeast (LILY) technology for *in vivo* labeling of yeast to produce eukaryotic lipid standards[15,16]. With our *in vivo* labeling approach several hundred stable-isotope-labeled lipids can be simultaneously produced enabling us to follow lipids as key players in fat cell differentiation. Isotope dilution approaches involving stable-isotope labeled lipid and metabolite standards can account for any error accumulated in the analytical chain of sample preparation, storage and measurement. Using such isotope dilution combination with high-end chromatography and MS instrumentation for the analysis of MSCs and adipocyte differentiation will provide us with enhanced data matrices as ideal starting point to build metabolic models. MSC differentiation affects numerous cellular metabolic pathways and signalling cascades. Mathematical metabolic models can reveal metabolic characteristics in these complex regulatory networks[17]. Based on such

genome-scale models, essential metabolites, lipids and proteins which are key to cell differentiation can be identified. For example, a genome-scale study on metabolic network model of bone marrow-derived MSCs has previously been presented[18]. A successful model was developed to identify ways to increase stem cell proliferation and differentiation, providing evidence for the key role of mathematical modelling in biomedical research. Thus, applying a combination of genome-scale modelling and experimental large-scale omics-analysis together with multivariate statistics or pattern recognition[19] promises to yield significant advance in the complex field of adipogenic differentiation.

The mechanistic understanding of fat cell development in the human body is essential for the treatment of obesity-related diseases. However, a high fraction of studies on the mechanisms that directs adipogenic differentiation rely on mouse models or murine cell lines [3,20–23]. In the context of cell-based therapies, translational aspects are of utmost importance as cells from different species might act differently. For example, the *in vitro* proliferation of human MSCs exhibits a relatively low frequency of oncogenic transformation in stark contrast to murine MSCs which frequently gain chromosomal defects *in vitro* and often produce fibrosarcomas when injected back into mice[5,24,25]. To enable potential translation of our results, we decided to use human primary MSCs in early passages for this study. In this work, we present a novel MS-based multiomics strategy to analyse adipogenesis in human MSCs relying on the combination of high-end MS and chromatography, isotopic dilution and network analysis.

2. Results

2.1. Development of a multiomics workflow for the analysis of adipogenic differentiation from MSCs

Primary adipose tissue-derived MSCs (MSC0) were cultivated in adipogenic differentiation medium for 21 days (MSC21). Successful adipogenic differentiation was observed by morphological changes of the cells and lipid vacuole formation (**Figure 1**). In order to perform a representative systems biology experiment the multiomics data should ideally be generated from the same set of samples to allow for direct comparison under the same conditions[26]. To meet these requirements, we applied (1) an adapted two-phase extraction procedure for MSC and fat cells (n=5) to sequentially extract lipids, metabolites and proteins[10]. The use of sequential lipid, metabolite and protein extraction provides the advantage of multimolecular information from one sample. We modified the orginal SIMPLEX protocol [10] by using nitrogen quenching so that trypsin was avoided and less amount of human MSCs and adipocytes (~10^5 cells) was needed. We developed a multiomics strategy based on hyphenated high-end mass spectrometry and chromatography for untargeted screening and targeted quantification. Protein information was generated by state of the art LC-MS/MS shotgun proteomics and was used to build metabolic networks linked to human genomic sequences. Metabolite and lipid profiling in MSCs and adipocytes was performed using a novel HILIC-RP dual injection strategy combined with high-resolution Orbitrap-MS[27]. Merging metabolomics and lipidomics assays is usually compromised by different extraction procedures needed (high polarity range from very polar small metabolites to medium-mass non-polar lipids) and that typically the two approaches deliver separate data sets. Using the parallel HILIC-RP method, metabolite and lipid information can be generated in parallel in one 32 min run. Concentrations ranging over 3–4 orders of magnitude can be assessed by the HILIC-RP-MS assay[27]. The addition of ^{13}C labeled metabolite/lipid standards enabled us to merge targeted quantification with untargeted compound screening in MSC0/21. Low sample amounts of MSCs and adipocytes (~ 10^5 cells) were needed detecting fmol absolute on column in the parallel HILIC-RP method. This is significantly lower than a recent shotgun lipidomics approach used for the quantitative analysis of white and brown adipose tissue, where pmol of lipids were theoretically detectable[36].

2.2. Targeted lipidomics and metabolomics comparing MSCs and adipocytes

For targeted analysis, we employed ^{13}C isotopically labeled metabolite and lipid standards produced in our laboratory for standardization[15,28,29] to follow fat cell differentitation of MSCs. Absolute compound-specific quantification of 12 lipids and 54 metabolites was performed using external calibration with internal standardization by in-house produced ^{13}C-labeled standards and protein normalization. All lipids and metabolites quantified in MSCs/adipocytes were in the range of nmol to fmol range per mg protein with limits of detection of fmol absolute on column. Isotope dilution and the use of the LILY lipids enhanced the quantification significantly (**Figure A1 and A2**) i.e. TG 54:6 (R^2 of 0.9812 vs. 0.7146 for label-free quantification). Once more showing the advantage of using our in-house produced standards for quantitation[15,30]. The comparision of the targeted metabolite and lipid quantification in MSCs and adipocytes revealed signficant downregulation (fold change > 2, p-value < 0.05) of GMP, S-adensoyl-methionine, asparagine, L-cystathionine, adenosine, 5'-deoxy-5'-methylthioadenosine and adenine in adipocytes. The amino acids showed a general trend to be less abundant in adipocytes (**Figure A3. A)**, whereas triglycerides and lipid precursors such as carnitine and propionyl-L-carnitine were increased upon differentiation (**Figure A3. B** and **C**), which can be explained by the formation of lipid droplets upon differentiation of the MSCs. Overall successful group separation in MSC and adipocytes could be performed by principal component analysis using the targeted metabolite and lipid data set (**Figure 2. A and B**).

2.3. Non-targeted lipidomics and metabolomics comparing MSCs and adipocytes

Non-targeted lipid and metabolite analysis revealed significant changes (fold change > 2, p-value < 0.05,) comparing undifferentiated MSCs (MSC0, cells before differentiation initiation) with MSCs differentiated into the adipogenic lineage (MSC21, cells after 21 days of adipogenic incubation). A general increase in molcular complexity in differentiated adipocytes was observed indicated by the higher number of identified metabolites and lipids (**Figure 3**). After filtering (Compound Discoverer 3.0: background removal using extraction and eluent blanks, area > 50 000, MetaboAnalyst: Interquartile range) and normalization (mean-centered and divided by the standard deviation of each variable in MetaboAnalyst), 171 compounds were significantly upregulated and 24 compounds were downregulated in adipocytes. Overall, 2650 compounds were identified in the lipid fraction of both sample groups which is three times higher compared to the metabolite fraction with 839 compounds. This observation reflects the formation of lipid droplets as a hallmark for adipogenic differentiation and is consistent with a general summed area increase in adipocytes detected for most of the abundant lipid classes nameley triglycerides (TG), phosphatidylcholine (PC), lysophosphatidylcholine (LPC), sphingomyelin (SM), ceramides (Cer), diglycerides (DG) (**Figure A4**). The upregulation was especially pronounced in TGs which are the main constituents of lipid droplets[3]. For the other major lipid classes detected, all belonging to the category of phospholipids, maintained levels (phosphatidylethanolamines-PE) or decreased lipid levels (phosphatidylserines-PS, phosphatidylinositols-PI, lysophosphatidylethanolamines-LPE) were observed indicating major phospholipid remodelling upon adipogenic differentiation and lipid droplet formation[31].

2.4. Biological validation and data interpretation of the multiomics workflow

2.4.1. Proteomics network reconstruction, metabolic modelling and pathway analysis

The shotgun proteomic analysis of non-differentiated and differentiated MSCs revealed significant dynamics of the cellular proteome during the differentiation process. Based on the human genome-scale consensus model Recon 2.4, proteomic data were applied to reconstruct context-specific networks which reflect the specific proteomic constitution of MSCs before and after differentiation. In total, 165 metabolic reactions and processes were fully reprogrammed on the proteome level during differentiation. Strongest effects were observed for reprogramming of reactions in fatty acid metabolism (oxidation, synthesis, eicosanoid, inositol phosphate and bile acid metabolism) and transport processes (peroxisomal, extracellular as well as endoplasmatic reticular transport) (**Figure A5**). Using the protein information together with the generated metabolite and

lipid (using a combination of targeted and non-targeted lists with median areas/concentrations for comparison of MSCS and adipocytes) data, multiomics pathway analysis (**Table S1**) was performed (OmicsNet[32]). Four different correlation networks revealed 113 signficantly regulated pathways (p-value > 0.05) comparing MSCs and adipocytes (**Table S2**). ATP and AMP showed the highest correlation degree (922, 141 respecitively) within the protein-metabolite network (**Figure 4. A + C**) due to the expected change in phosphorylation-dephosphorylation and energy metabolism upon fat differentiation[11]. Several interesting and expected active pathways were identified (**Figure 4. A-C**) such as (1) glycerophospholipid signaling (**Figure 4. A+B**)[10,33], (2) the insulin pathway (**Figure 4. C**)[8–10], (3) glycerolipid (triglycerides regulating) pathway with corresponding fat digestion and absorption (LPL protein (**Figure A6.A**)[11,34,35], (4) carnitine regulation within the fatty acid metabolism, PPAR signaling and adipocytokine signaling pathways (**Figure A6.B**)[36–38] and (5) gluthatione disulfide within arachidonic acid metabolism and oxidation related pathways[39–41].

2.4.2. Carnitine regulation

Increased concentrations of carnitine and propionyl-L-carnitine were observed in adipocytes by targeted analysis (**Figure A3. C, Figure A6. B)**. Carnitine synthesis is necessary for fatty acid oxidation and fatty acid transport from the cytsosol to the mitochondria[42] and is known to improve insulin sensitivity of adipocytes[43], an inherent characteristic of adipose tissue. Interestingly, upregulated acyl-carnitine levels are associated to promote the differentiation process of embryonic stem cell in different cell types[39]. Additionally, carnitine and acetylcarnitine were found to reduce adipogenesis but stimulate osteogenesis and chondrogenesis in human MSCs by regulating the mitochondrial metabolisms [36]. It is also known to attenuate lipid accumulation in adipocytes via downregulation of PPARγ, a major adipocyte-specific transcription factor[44].

2.4.3. Trigylcerides upregulation in lipid droplets of adipocytes

Major increase of TGs in adipocytes was observed in the targeted lipid analysis (**Figure A3. B**) and number of identifications received by non-targeted lipidomics (**Figure 3**). Comparing the 10 most regulated compounds in the classes of MSCs and adipocytes (from the combined untargeted metabolite and lipid data set), several interesting m/z variables were found by partial least square and heat map analysis (MetaboAnalyst 4.0). Some of them could be further identified by database search (Lipid Search) and manual curation. Four upregulated triglycerides in adipocytes were annotated based on acuurate mass, fragmentation and retention time namely TG (16:0_16_1_18:0), TG (16:0_16:1_18:1), TG (16:1_18_0_18_0) and TG (16:0_18:1_18:1). TGs are the major constituents of lipid droplets representative for successful adipogenic differentiation. Expected lipid droplet formation was induced in the adipocytes (**Figure 1**) upon medium change and reflected in the list of regulated proteins by the increase of e.g. fatty acid synthase, glycerol-3-phosphate dehydrogenase, and malic enzyme which are all known to increase the triglyceride metabolism[11].

2.4.4. Gangliosides are involved in adipocyte differntation and insulin sensisity

The m/z for the gangliosides GM3(d18:1/16:0) and GM3(d18:1/22:1) were listed the 10 most regulated compounds identified (partial leat square, heat map, MetaboAnalyst) comparing MSCs and adipocytes. We annotated them manually by m/z, fragmentation and matching retention times (in positive and negative MS mode) and upregulation by a factor of 20 and 30 respectively was observed in adipocytes. Comparing the ganglioside glycosphingolipid fragmentation pattern (**Figure A7**), the ceramide moiety was determined in the positive ion mode (characteristic sphingosine fragments at m/z 264 and 282) and the glycan residue was annoated in the negative ion mode (characteristic N-acetylneuraminic acid fragment ion at m/z 290). Additionally, a series of gangliosides (GM3(32:1;2) GM3(32:0;2), GM3(33:1;2), GM3(34:0;2), GM3(34:2;2), GM3(35:1;2) , GM3(36:0;2), GM3(36:1;2), GM3(36:2;2), GM3(38:1;2), GM3(40:0;2), GM3(40:1;2), GM3(40:2;2), GM3(41:0;2), GM3(41:1;2), GM3(41:2;2), GM3(42:0;2), GM3(42:1;2), GM3(43:1;2), GM3(43:2;2)) was identified by m/z, elution order depending on number of double bonds, fatty acid chain length as

Preprints (www.preprints.org) | NOT PEER-REVIEWED | Posted: 2 September 2019 doi:10.20944/preprints201909.0017.v1

Peer-reviewed version available at Molecules 2019, 24, 3615; doi:10.3390/molecules24193615

well as matching retention time (elution: 22.3-28.3 min) between the different MS modes (+/-). Ten (GM3(33:1;2), GM3(35:1;2) , GM3(36:0;2), GM3(41:0;2), GM3(41:1;2), GM3(41:2;2), GM3(42:0;2), GM3(42:1;2), GM3(43:1;2), GM3(43:2;2)) of the 22 identified gangliosides were only found in adipocytes and all other gangliosides were found in lower abundance in MSCs. This is of special interest, as GM3 gangliosdes are part of the sphingolipid metabolism identified by protein-metabolite network data (**Figure S2**). Gangliosides were proposed as a new class of stem cell markers e.g. GD1a increase for favored osteogenesis in MSCs[45]. They were further found to be involved in the differentiation of MSCs into osteoblasts and neural cells[46] and are generally associated with the insulin metabolic signaling in adipocytes[47]. Insulin is required for fat cell formation activating distinct signal transduction pathways, such as phosphorylation-dephosphorylation or the phosphatidylinositol 3-kinase pathway[10]. Major reprogramming of related pathways (insulin, glycerolipid, sphingolipid, phosphatidylinositol pathway) was also confirmed by the multiomics data (**Figure 4, Supplementary data A2, Figure B5**). Additionally, we observed upregulation of perilipin-4 upon adipocyte differentiation of MSCs which is an adipocyte phosphoprotein present in the periphery of lipid storage droplets[3,11].

2.5. Figures

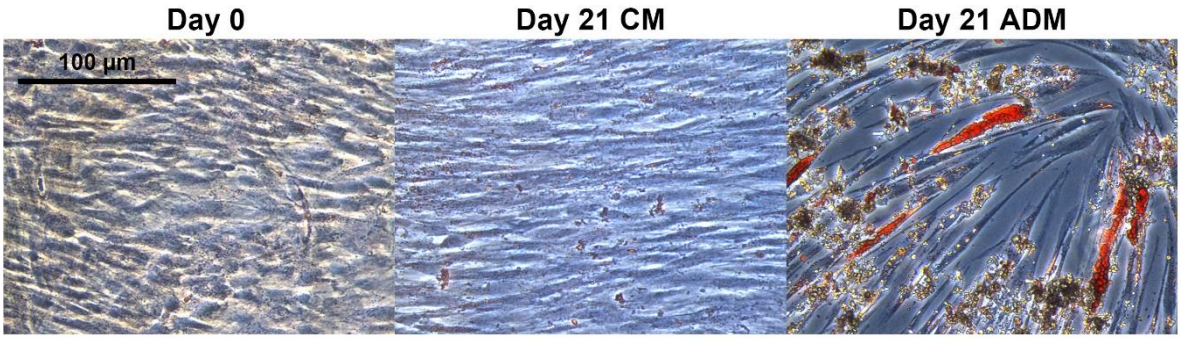

Figure 1. Oil Red O staining of adipose tissue-derived MSCs after 0 and 21 days cultivation in adipogenic differentiation medium (ADM) or control medium (CM). Scale bar indicates 100 µm

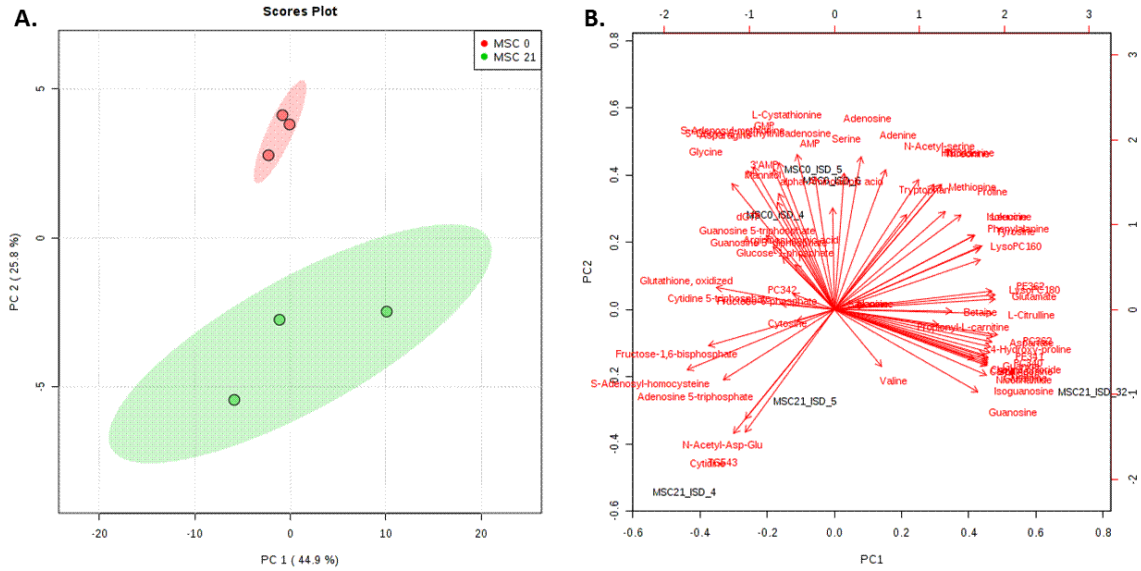

Figure 2: Principal component analysis for the targeted lipid and metabolite analysis comparing MSCs and adipocytes. All compounds were quantified (54 metabolites, 12 lipids) using compound-specific quantification with 13C labeled yeast extract. A. PCA score plots in MetaboAnalyst 4.0[48] explaining most (71%) of the variance by PC 1 and PC 2 showing successful separation of the MSCs (MSC0) and adipocytes (MSC21). B. Biplot (MetaboAnalyst) including the loading information of the individual metabolites/lipids.

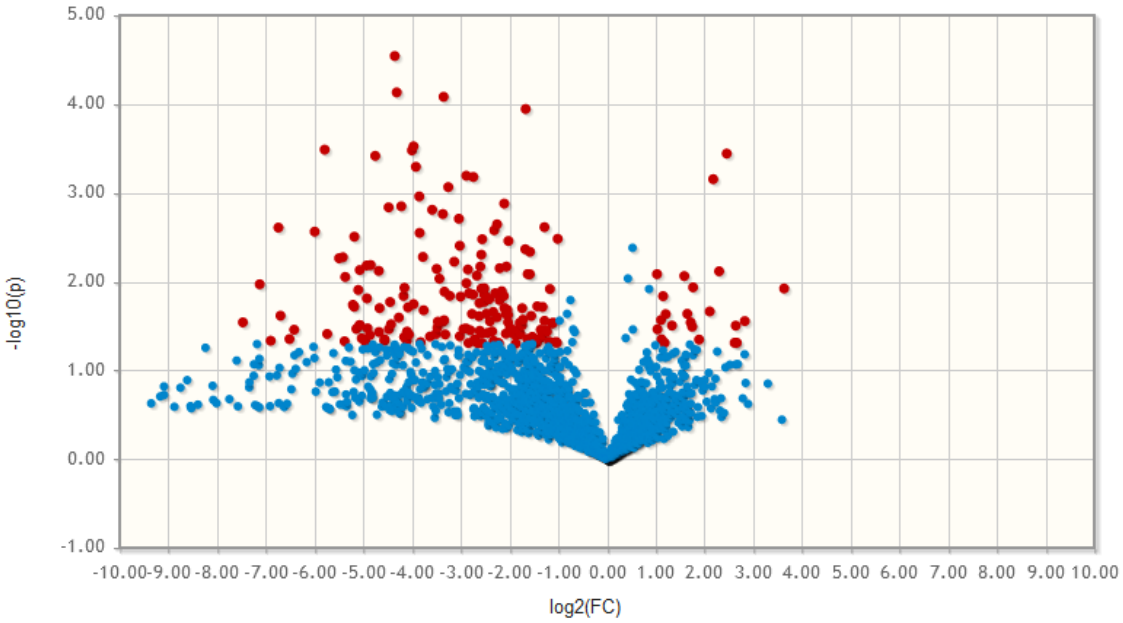

Figure 3. Differential analysis of lipids and metabolites. Volcano plot (derived from untargeted LC-MS) of compounds from primary MSCs and adipocytes using MetaboAnalyst 4.0 (with p-value settings 0.05, interquartile filter)[48]. HILIC-RP-HRMS (positive mode) revealed that 355 out of 7732 compounds were significantly regulated (p-value < 0.05, fold change (FC) >2). Both lipids and metabolites were significantly upregulated in adipocytes compared to MSCs.

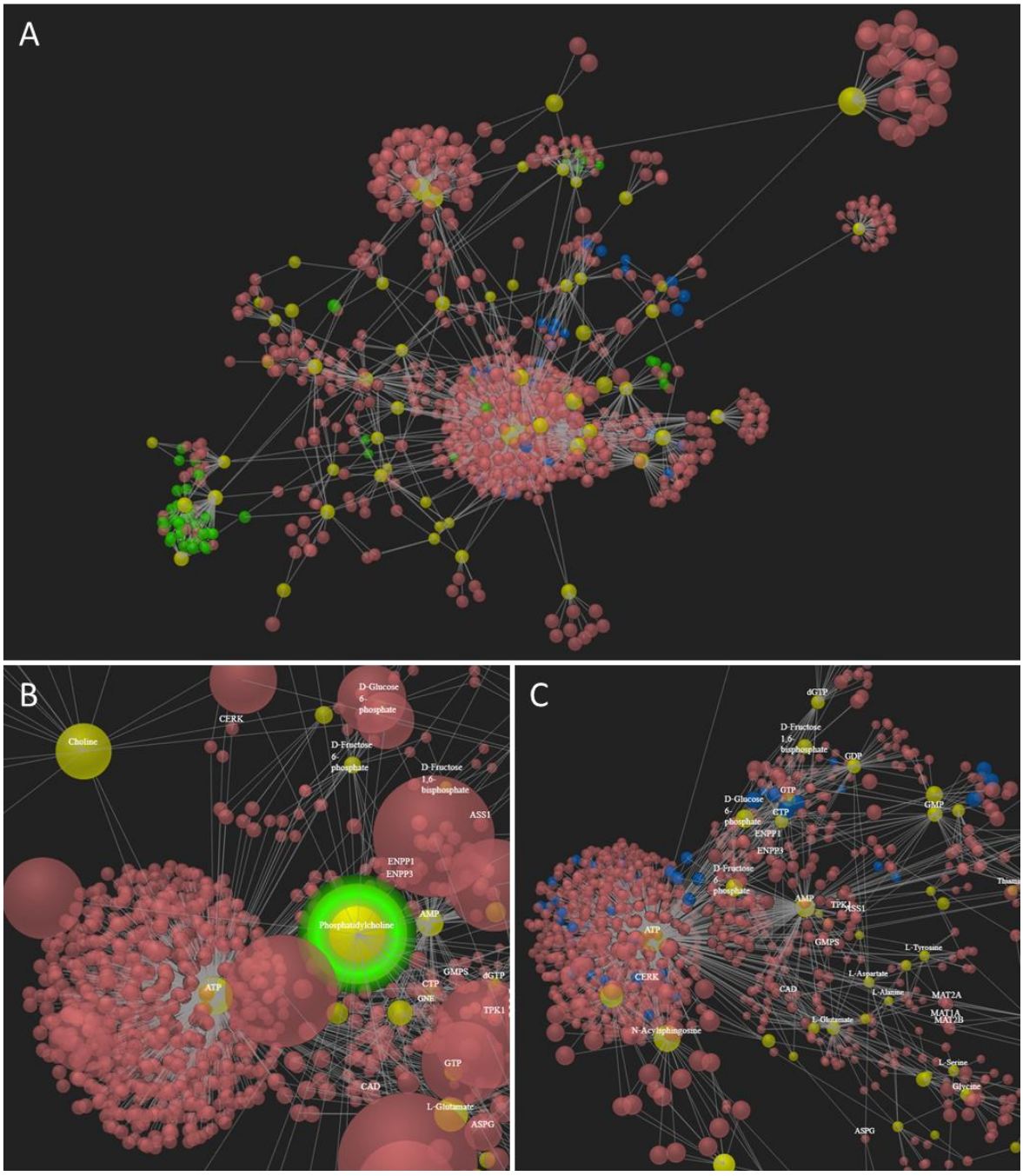

Figure 4. Multiomics network analysis of MSCs and adipocytes. Network analysis enabled to combine protein, metabolite and lipid information and identify regulated pathways in adipogenesis. A. Network including most protein-metabolite interactions. Proteins are labeled in red, metabolites in yellow. The glycerophospholipid metabolism is labeled in green and the insulin pathway in blue. B. Phosphatidylcholine as regulated lipid within the glycerophospholipid metabolism. C. ATP and AMP as major regulated energy metabolites, additionally the insulin pathway is significantly regulated and labeled in blue.

3. Discussion

The presented multiomics study on the adipogenic differentiation of MSCs is a proof of principle for the power of multimolecular extraction procedures combined with orthogonal LC-MS assays and network construction. Merging metabolomics and lipidomics assays was possible by adapting (no trypsin, less starting cell number) the original SIMPLEX protocol [10] for sequential lipid, metabolite and protein extraction. Followed by the HILIC-RP dual injection setup, metabolite and lipid information was generated from the same sample in one analytical run. Additionally,

targeted quantification by ^{13}C labeled metabolite/lipid standards could be performed with untargeted compound screening in the same assay so that sample amounts needed were significantly reduced. LC-MS assays are especially useful when low abundant metabolites and lipids are of interest as the chromatographic separation offers cleanup of the sample matrix, higher linear dynamic range and additional compound identification by retention time information. The power for the detection of unknown low abundant compounds was impressively shown by the example of GM3 gangliosides in MSCs and adipocytes. None of the gangliosides could be annotated by data base search although the used in silico database included all types of gangliosides (GM1, GM2, GM3). Only when comparing the non-targeted datasets of MSCs and adipocytes, two of these high mass (> 1000 m/z) glycosphingolipids showed up as interesting differentiating unknown compound. Using manual curation of the fragmentation pattern, matching retention times in the positive and negative ion mode and retention time order, 22 different gangliosides could be successfully annotated. All biological observations for the regulation of triglycerides[3,8], gangliosides[47] and reprogrammed pathways[23] in adipocytes are in accordance with literature. Further biological interpretation of the data is beyond the scope of this work. Future studies will focus on in-depth analysis of fat differentiation involving time-series experiments, tracer studies and the comparison of different fat cell tissue types. Additionally, targeted LC-MS based assays will be developed for metabolite and lipid classes relevant in adipogenesis such as triglycerides, acyl-carnitines or gangliosides.

The presented biotechnology workflow based on adult human MSCs from surgical waste represents a general strategy to avoid animal experiments and induced pluripotent stem cells[6,49] for certain clinical studies and drug testing. The performed biological validation (literature search, identification of relevant regulated compounds and pathways) combined with the analytical method validation (analytical figures of merit; use of commercially available standards as well as in-house produced labeled metabolites and lipids; database annotation based on RT, accurate mass and fragmentation pattern; additional manual curation), let us conclude that the presented workflow is fit for purpose for other cell culture or tissue-based multiomics studies. Our multiomics workflow enables the generation of comprehensive multimolecular information based on a single sample (using the sequential extraction approach) and low analysis time. We hypothesize that reproducible diagnostic high-throughput LC-MS based assays can be implemented by automatic sample extraction and data evaluation.

4. Materials and Methods

4.1. Cell culture

The use of human tissue was approved by the ethics committee of the Medical University Vienna, Austria (EK Nr. 957/2011, 30 January 2013) and the donor gave written consent. Human adipose tissue-derived MSCs were isolated from a female donor (age 29) within 3 - 6 h after surgery as described before[50]. Briefly, adipose tissue was obtained from abdominoplasty, minced with scissors and digested with collagenase type I (Sigma Aldrich, St. Louis, MO, USA). After several centrifugation and washing steps, the stromal vascular fracture was released in a cell culture flask (Sarstedt, Nümbrecht, Germany) with standard cell culture medium composed of MEM alpha (Thermo Fisher Scientific, Waltham, MA, USA), 0.5% gentamycin (Lonza, Basel, Switzerland), 2.5% human platelet lysate (hPL; PL BioScience, Aachen, Germany), and 1 U/mL heparin (Ratiopharm, Ulm, Germany) and incubated in a humidified incubator at 37 °C and 5% CO_2. Subsequently, MSCs were selected by plastic adherence and cryo-preserved in 77.5 % MEM alpha, 12.5% hPL, 10% DMSO (Sigma Aldrich), and 1 U/ml heparin (defined as passage 0, P0). For the adipogenic differentiation, cells were thawed at passage 0 and further expanded for two passages in T-flasks. After harvest via accutase (GE healthcare, Little Chalfont, UK) treatment, MSCs were seeded at 4.000 cells/cm^2 in a 6-well plate (Sarstedt), coated with 2 µg/cm^2 fibronectin (Sigma) and 2 ml of CM was added. Upon confluency, the medium was changed to adipogenic differentiation medium (ADM; Miltenyi, Bergisch-Gladbach, Germany), supplemented with 0.5% gentamycin, and the cells were cultured for 21 days, while the medium was

changed every 2 – 3 days. Undifferentiated MSCs at day 0 served as control. Subsequently, the cells were fixed with 4% paraformaldehyde (Sigma), washed with ddH_2O and stained with Oil Red O solution (Sigma). The staining of lipid vacuoles was observed by bright-field microscopy (DMIL LED with camera ICC50HD; both Leica, Wetzlar, Germany).

4.2. Multiomics

All solvents were LC-MS grade. Metabolite and lipid standards were from Sigma, Carbosynth (Berkshire, UK) or Avanti Polar Lipids, Inc. (Alabama,USA) and were weighed and dissolved in an appropriate solvent. A multi-metabolite mix (x metabolites) and multi-lipid mix (x lipids) were prepared. A metabolite and lipid ^{13}C labeled standard was prepared using the fully ^{13}C labeled internal standard from ISOtopic solutions e.U. (Vienna, Austria), combined with an in-house produced ^{13}C labeled lipid LILY fraction and reconstituted in 50% MeOH. All cell samples (n=5) and medium blanks (n=2) were quenched with liquid nitrogen prior to storage at -80°C until sample preparation. The adherent cells (~10^5 per sample) were harvested using a cell scraper and extracted with a mixture of methanol, methyl-tert-butylether and 10 mM ammonium formate. The adapted SIMPLEX two-phase extraction preparation[10] enabled the collection of the lipid fraction (upper phase), the metabolite fraction (lower phase) and the protein pellet. Part of the samples were spiked (n=3) with ^{13}C-isotopically labeled metabolites and LILY lipids for quantification.

A novel HILIC-RP DUAL injection strategy combined with high-resolution Orbitrap-MS was applied for the simultaneous analysis of small polar metabolites and lipids[27] of the MSC samples. Briefly, a Vanquish Duo UHPLC system (Thermo Fisher Scientific) equipped with an autosampler with two injection units, two binary pumps and a column compartment was used to enable parallel HILIC and RP analyses. A SeQuant® ZIC®-pHILIC column (150 × 2.1 mm, 5 µm, polymer, Merck-Millipore) was used with gradient elution under alkaline conditions (mobile phase A: 90% 10 mM ammonium bicarbonate, pH 9.2/10% ACN; mobile phase B 100% ACN) combined with a an Acquity HSS T3 (2.1 mm × 150 mm, 1.8 µm, Waters) RP column (mobile phase A: ACN/H2O 3 : 2, v/v, solvent B: IPA/ACN 9 : 1, v/v) using a VanGuard Pre-column (2.1 mm × 5 mm, 100 Å, 1.8 µm). Two different gradients were applied for HILIC and RP with a total run time of 32 min as described before[27] using a flow rate of 250 µL min^{-1} and an injection volume of 5 µL. An additional 2-positional 6-port valve and the use of a T-piece in front of the mass spectrometer enabled to deliver the HILIC (0-11 min) or RP (11-32 min) eluent to the MS, while the other separation eluent was directed to waste. High-resolution mass spectrometry in positive and negative mode was conducted on a high field Thermo Scientific™ Q Exactive HF™ quadrupole- Orbitrap mass spectrometer equipped with an electrospray source using Full-MS (resolution 120 000 for quantification, positive mode only) and ddMS (resolution 30 000, positive and negative mode) for identification.

The protein fractions containing the isotopically spiked samples (n=3) were determined by Bradford assay (Pierce™ Coomassie Plus Assay Kit) and used for normalization. The other protein fraction (n=2) was used for shotgun proteomics including protein extraction, digestion and LC-MS/MS analysis was applied. Proteins were extracted in a guanidine chloride/HEPES buffer followed by precipitation in methanol/chloroform/water mixture. After reduction and alkylation, proteins were trypsin digested over-night and 1µg was loaded on the column for LC-MS/MS analysis.

4.3. Data analysis

Data analysis was performed by dedicated software for targeted (Skyline, Tracefinder 4.1) and untargeted analysis (metabolites: XC-MS, Compound Discoverer; lipids: Lipid Data Analyzer, Lipid Search 4.1; proteins: compound discoverer). Further statistical and pathway analysis was performed using MetaboAnalyst 4.0[48]. Adipocyte samples had a higher variation than MSC cells, which was considered for statistical analysis. Context-specific metabolic networks were reconstructed from shotgun proteomics data applying the FASTCORE algorithm[51] using a consistent version of Recon 2.4[52]. FASTCC[51] was applied with the default flux activity threshold of 1e-4. Proteomic data was mapped to the consistent version of Recon2.4 via the Gene Protein Association rules (GPR rules) to obtain a set of core reactions, i.e. reactions that were found both in the proteomic data and the network

model of Recon2.4. FASTCORE was used to identify the missing reactions necessary to obtain a consistent context-specific subnetwork for all differentiation states. OmicsNet was used for multiomics data integration , visualization and pathway analysis[32].

Supplementary Materials: The following are available online at www.mdpi.com/xxx/s1, Table S1. Protein and metabolite list, Table S2. Regulated pathways comparing MSC and adipocytes.

Author Contributions: Conceptualization, E.R., D.E and T.N.; methodology, E.R, M.R., H.S., and G.K.; software, E.R, T.N. and M.R.; validation, E.R., T.N. and D.E.; investigation, E.R. and H.S.; resources, G.K, C.K. and T.N.; data curation, E.R, M.P.P, G.M., T.N..; writing—original draft preparation, E.R.; writing—review and editing, E.R. D.E., T.N., G.K, and C.K.; project administration, E.R.; funding acquisition, E.R., D.E., C.K., G.K and T.N.

Funding: The LILY project for the production of isotopically labeled lipid received funding from the Austrian BMWFW Federal Ministry (aws PRIZE prototype funding).

Acknowledgments: This work is supported by the University of Vienna, the Faculty of Chemistry, the Vienna Metabolomics Center (VIME; http://metabolomics.univie.ac.at/) and the research platform Chemistry Meets Microbiology and the Mass Spectrometry Center (MSC) of the University of Vienna. The authors thank all members of individual groups (University of Vienna, University of Natural Resources and Life Sciences and LMU München) for continuous support. Especially, we acknowledge Sophie Neumayer for laboratory and Yasin El Abiead for data evaluation discussion.

Conflicts of Interest: The authors declare no conflict of interest.

Appendix A

Table S1. **Protein and metabolite list**. Input list of identified proteins (fasta numbers), lipids and metabolites (human metabolome database numbers) using median areas/concentrations for MSCs and adipocytes.

Table S2. Regulated pathways comparing MSC and adipocytes. Significantly regulated (p-value < 0.05) pathways identified by protein/metabolite network interaction using OmicsNet[32].

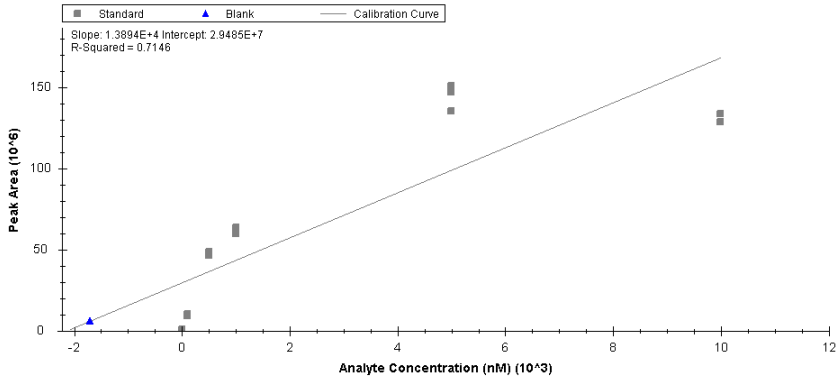

Figure A1: TG 54:6 label-free quantification using external calibration

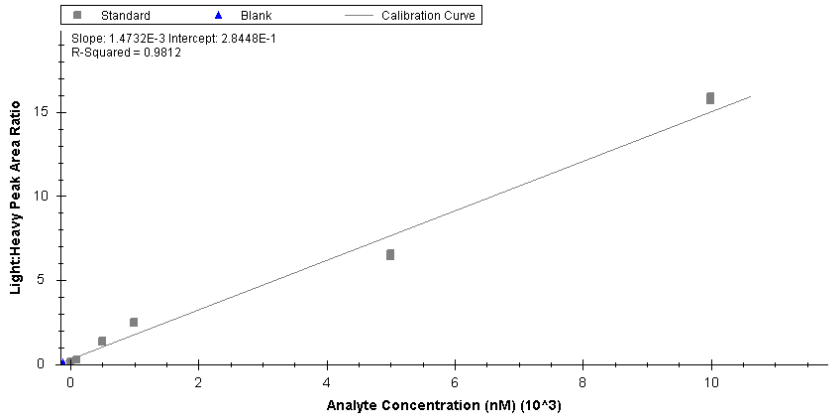

Preprints (www.preprints.org) | NOT PEER-REVIEWED | Posted: 2 September 2019 doi:10.20944/preprints201909.0017.v1

Peer-reviewed version available at Molecules 2019, 24, 3615; doi:10.3390/molecules24193615

Figure A2: Compound-specific quantification of TG 54:6 using external calibration and internal standardization by ^{13}C-labeled TG 54:6 (LILY technology[15]).

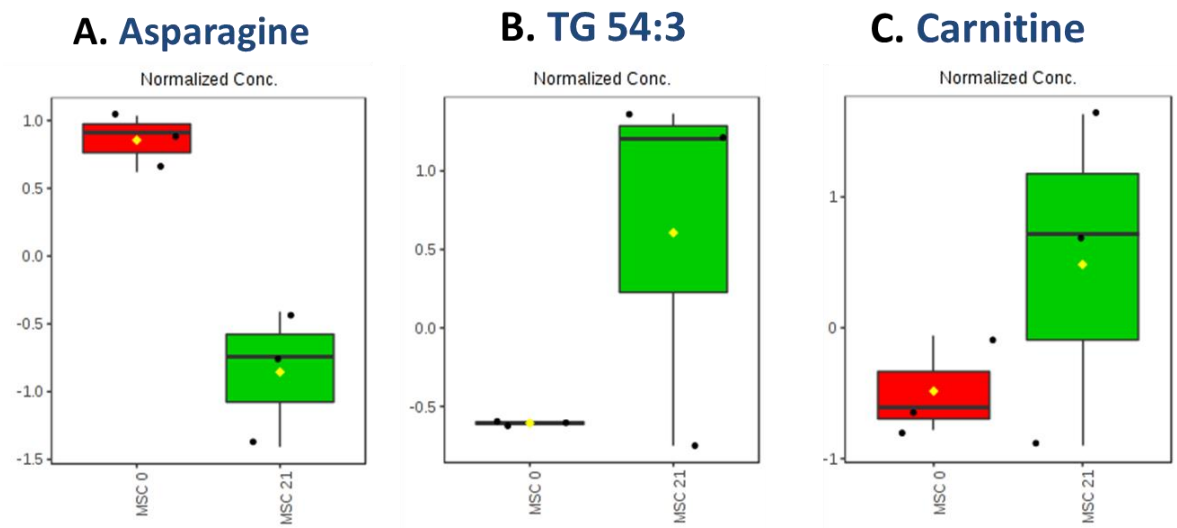

Figure A3: Exemplary targeted quantification of metabolites and lipids. Compound-specific quantification in MSCs (MSC0) and adipocytes (MSC21) using external calibration and standardization by ^{13}C-labeled matching compounds for A. normalization was performed by protein amounts and autoscaling in MetaboAnalyst 4.0[48]. For amino acids such as asparagine general downregulation in adipocytes was observed. For lipids and lipid precursors such as TG 54:3 (B.) or carnitine (C.) a trend towards upregulation in adipocytes was observed.

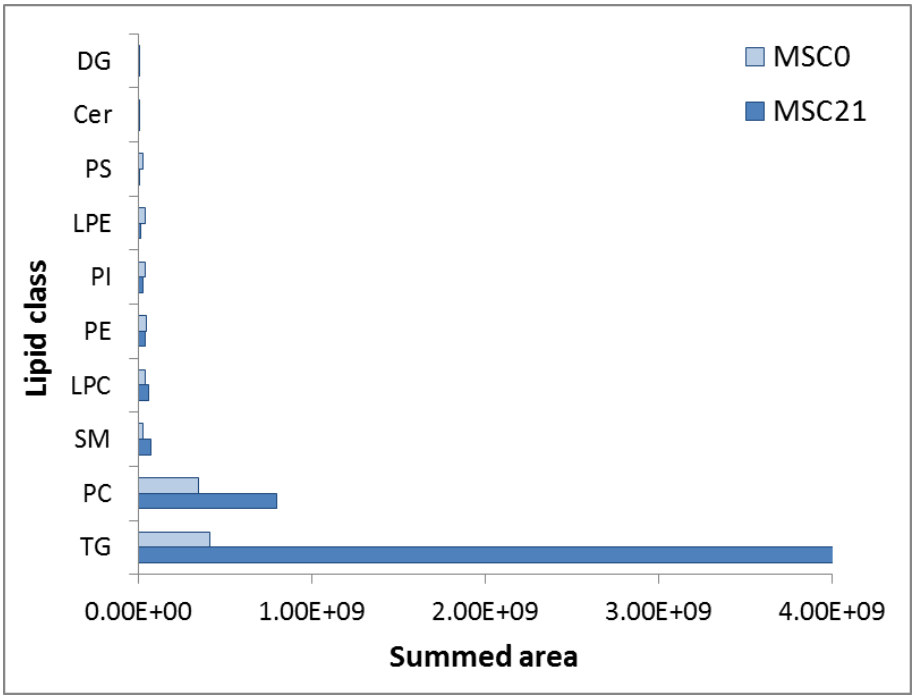

Figure A4. **Most abundant lipid classes in MSCs and adipocytes**. Identification was performed with LipidSearch 4.2. using the summed areas of all annotated lipids in a given lipid class. Abbreviations: DG- Diglyceride, Cer- Ceramide, PS- Phosphatidylserine, LPE- Lysophosphatidylethanolamine, PI- Phosphatidylinositol, PE- Phosphatidylethanolamine, LPC- Lysophosphatidylcholine, SM- Sphingomyline, PC- Phosphatidylcholine, TG- Triglyceride

Preprints (www.preprints.org) | NOT PEER-REVIEWED | Posted: 2 September 2019 doi:10.20944/preprints201909.0017.v1

Peer-reviewed version available at Molecules 2019, 24, 3615; doi:10.3390/molecules24193615

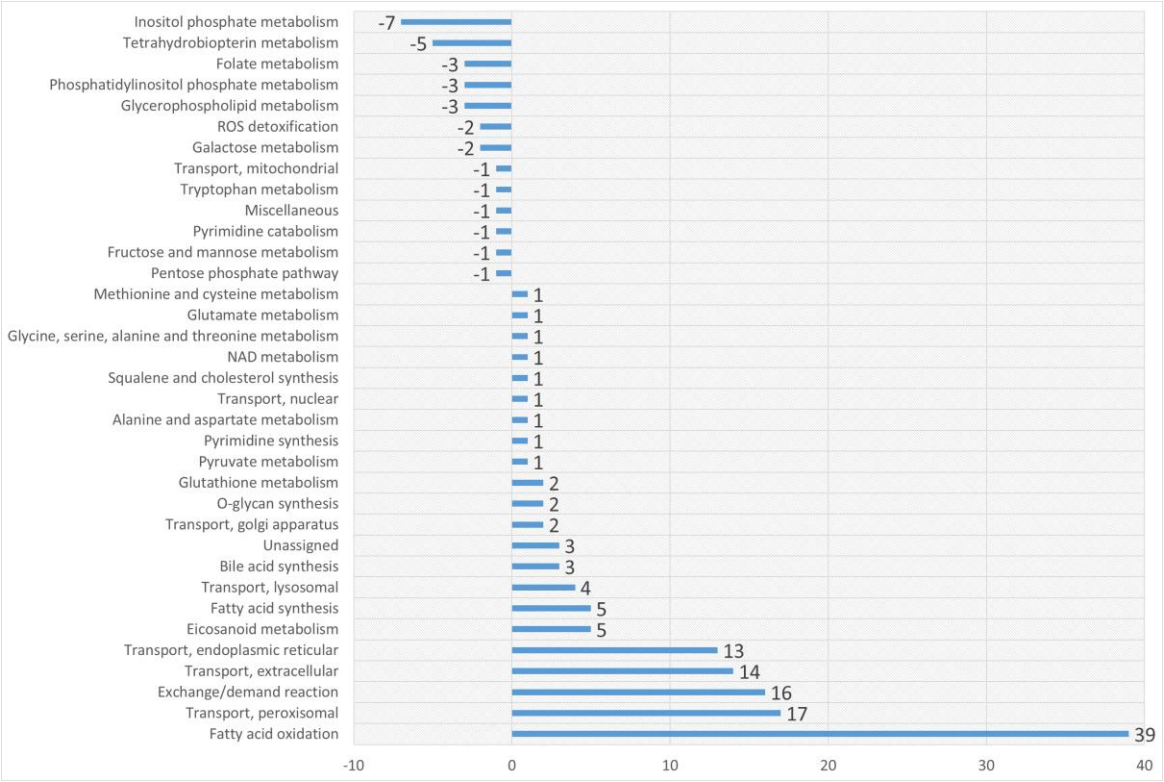

Figure A5. **Reprogramming of metabolic pathways during adipogenic differentiation of MSCs**. Numbers represent differences of proteomics-based reconstructed pathways before and after MSC differentiation. A positive number indicates an increase of reactions in the pathway during differentiation, negative numbers indicate a decrease during differentiation. Differences were built from mean values of two replicates.

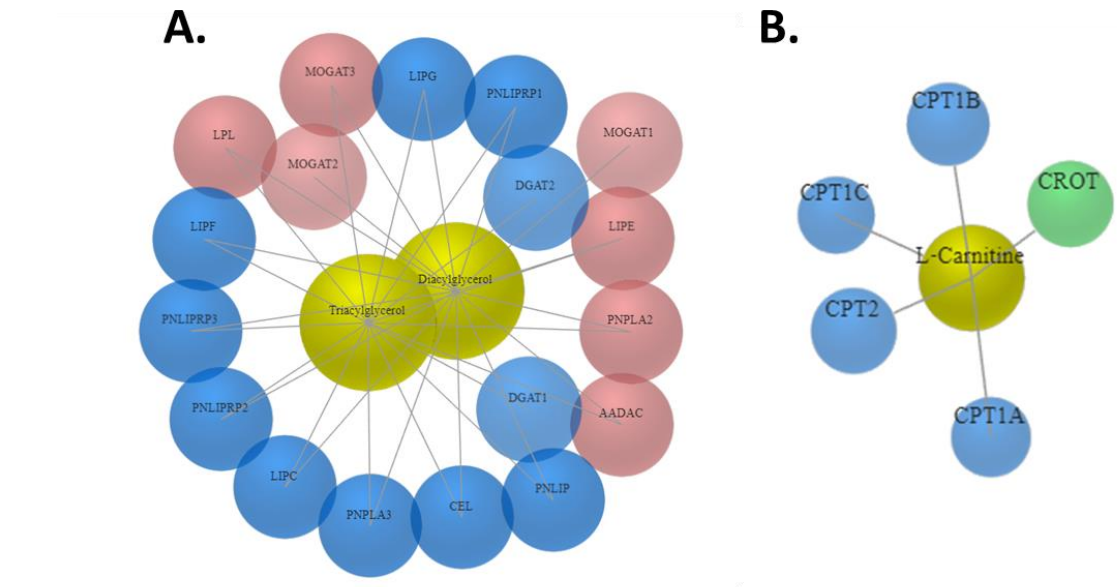

Figure A6. **Carnitine and di- and triglyceride regulation in adipogenic differentiation**. Example networks of metabolite-protein interaction analysis using OmicsNet[32] **A.** Triglyceride and diglyceride regulation in adipocytes. The blue labeling highlights the glycerophospholipid proteins. **B.** Carnitine network. The blue labeling highlights proteins of the PPAR signaling pathway, green label of CROT: Transport of medium- and long- chain acyl-CoA molecules out of the peroxisome to the cytosol and mitochondria. The protein thus plays a role in lipid metabolism and fatty acid beta-oxidation.

Preprints (www.preprints.org) | NOT PEER-REVIEWED | Posted: 2 September 2019 doi:10.20944/preprints201909.0017.v1

Peer-reviewed version available at Molecules 2019, 24, 3615; doi:10.3390/molecules24193615

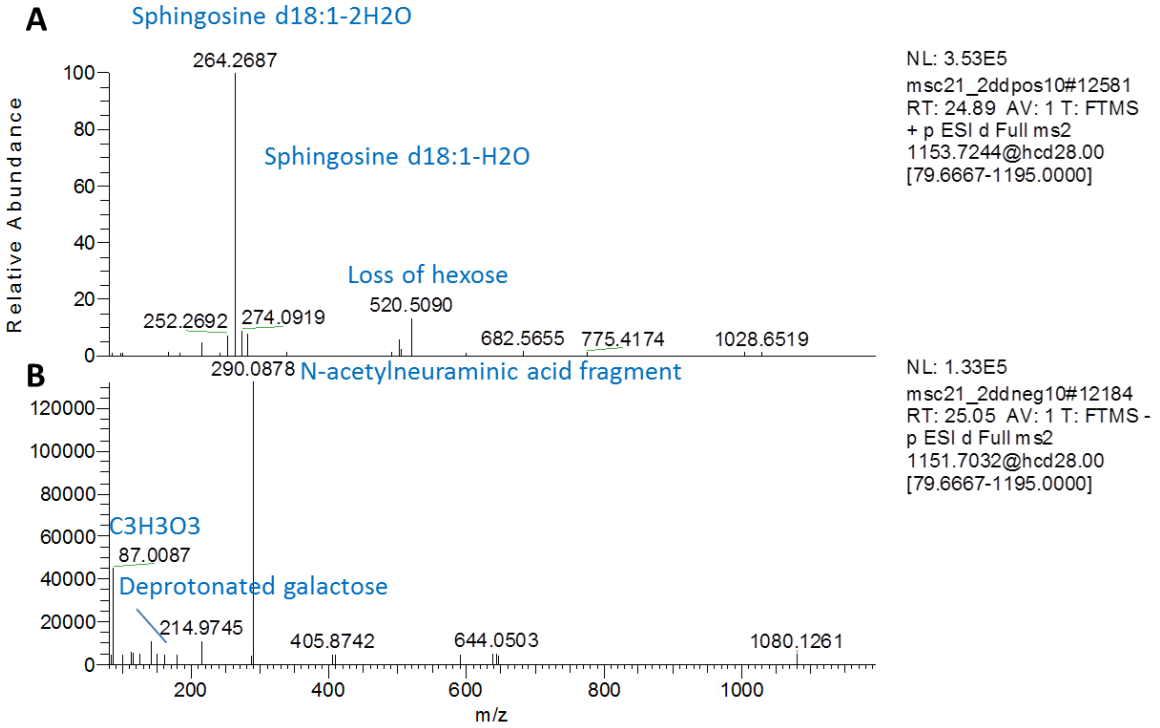

Figure A7: MS2 spectra of predicted ganglioside. Fragmentation spectra (Thermo Xcalibur) of regulated ganglioside GM3(d18:1/16:0) (sum formula, $C_{57}H_{104}N_2O_{21}$) show characteristic lipid fragments in the positive ion mode and characteristic glycan moieties in the negative ion mode

References

1. Tang, Q.Q.; Lane, M.D. Adipogenesis: From Stem Cell to Adipocyte. *Annu. Rev. Biochem.* **2012**, *81*, 715–736.
2. Gimble, J.M.; Katz, A.J.; Bunnell, B.A. Adipose-derived stem cells for regenerative medicine. *Circ. Res.* **2007**, *100*, 1249–1260.
3. Galateanu, B.; Dinescu, S.; Cimpean, A.; Dinischiotu, A.; Costache, M. Modulation of adipogenic conditions for prospective use of hADSCs in adipose tissue engineering. *Int. J. Mol. Sci.* **2012**, *13*, 15881–15900.
4. Dai, R.; Wang, Z.; Samanipour, R.; Koo, K.; Kim, K. Adipose-Derived Stem Cells for Tissue Engineering and Regenerative Medicine Applications. *Stem Cells Int.* **2016**, *2016*, 1–19.
5. Fitzsimmons, R.E.B.; Mazurek, M.S.; Soos, A.; Simmons, C.A. Mesenchymal stromal/stem cells in regenerative medicine and tissue engineering. *Stem Cells Int.* **2018**, *2018*.
6. Yoshihara, M.; Hayashizaki, Y.; Murakawa, Y. Genomic Instability of iPSCs: Challenges Towards Their Clinical Applications. *Stem Cell Rev. Reports* **2017**, *13*, 7–16.
7. Badimon, L.; Cubedo, J. Adipose tissue depots and inflammation: Effects on plasticity and residentmesenchymal stem cell function. *Cardiovasc. Res.* **2017**, *113*, 1064–1073.
8. Wu, Z.; Rosen, E.D.; Brun, R.; Hauser, S.; Adelmant, G.; Troy, A.E.; McKeon, C.; Darlington, G.J.; Spiegelman, B.M. Cross-regulation of C/EBPα and PPARγ controls the transcriptional pathway of adipogenesis and insulin sensitivity. *Mol. Cell* **1999**, *3*, 151–158.
9. Park, B.O.; Ahrends, R.; Teruel, M.N. Consecutive Positive Feedback Loops Create a Bistable Switch that Controls Preadipocyte-to-Adipocyte Conversion. *Cell Rep.* **2012**, *2*, 976–990.
10. Coman, C.; Solari, F.A.; Hentschel, A.; Sickmann, A.; Zahedi, R.P.; Ahrends, R. Simultaneous Metabolite, Protein, Lipid Extraction (SIMPLEX): A Combinatorial Multimolecular Omics Approach for Systems Biology. *Mol. Cell. Proteomics* **2016**, *15*, 1453–1466.
11. Gregoire, F.M.; Smas, C.M.; Sul, H.S. Understanding adipocyte differentiation. *Physiol. Rev.* **1998**, *78*, 783–809.
12. Fell, D.A. Beyond genomics. *Trends Genet.* **2001**, *17*, 680–682.
13. Fiehn, O.; Fiehn O Metabolomics–the link between genotypes and phenotypes. *Plant Mol. Biol.* **2002**, *48*, 155–71.
14. Griffiths, W.J.; Wang, Y.; Bill, W. Mass spectrometry : from proteomics to metabolomics and lipidomics w. **2009**, 1882–1896.
15. Rampler, E.; Coman, C.; Hermann, G.; Sickmann, A.; Ahrends, R.; Koellensperger, G. LILY-lipidome isotope labeling of yeast: in vivo synthesis of 13 C labeled reference lipids for quantification by mass spectrometry. *Analyst* **2017**, *142*, 1891–1899.
16. Rampler, E.; Criscuolo, A.; Zeller, M.; El Abiead, Y.; Schoeny, H.; Hermann, G.; Sokol, E.; Cook, K.; Peake, D.A.; Delanghe, B.; et al. A Novel Lipidomics Workflow for Improved Human Plasma Identification and Quantification Using RPLC-MSn Methods and Isotope Dilution Strategies. *Anal. Chem.* **2018**, *90*, 6494–6501.
17. He, Y.; Wang, Y.; Zhang, B.; Li, Y.; Diao, L.; Lu, L.; Yao, J.; Liu, Z.; Li, D.; He, F. Revealing the metabolic characteristics of human embryonic stem cells by genome-scale metabolic modeling. *FEBS Lett.* **2018**, *592*, 3670–3682.
18. Fouladiha, H.; Marashi, S.A.; Shokrgozar, M.A.; Farokhi, M.; Atashi, A. Applications of a metabolic network model of mesenchymal stem cells for controlling cell proliferation and differentiation.

Cytotechnology **2018**, *70*, 331–338.

19. Fürtauer, L.; Pschenitschnigg, A.; Scharkosi, H.; Weckwerth, W.; Nägele, T. Combined multivariate analysis and machine learning reveals a predictive module of metabolic stress response in Arabidopsis thaliana. *Mol. Omi.* **2018**, *14*, 437–449.
20. Simon, M.F.; Daviaud, D.; Pradère, J.; Guigné, C.; Wabitsch, M.; Chun, J.; Valet, P.; Saulnier-Blache, J.S. Lysophosphatidic acid inhibits adipocyte differentiation via lysophosphatidic acid 1 receptor-dependent down-regulation of peroxisome proliferator-activated receptor gamma2. *J. Biol. Chem.* **2005**, *280*, 14656–62.
21. Shoham, N.; Girshovitz, P.; Katzengold, R.; Shaked, N.T.; Benayahu, D.; Gefen, A. Adipocyte stiffness increases with accumulation of lipid droplets. *Biophys. J.* **2014**, *106*, 1421–1431.
22. Silva, F.J.; Holt, D.J.; Vargas, V.; Yockman, J.; Boudina, S.; Atkinson, D.; Grainger, D.W.; Revelo, M.P.; Sherman, W.; Bull, D.A.; et al. Metabolically active human brown adipose tissue derived stem cells. *Stem Cells* **2014**, *32*, 572–581.
23. Nassiri, I.; Lombardo, R.; Lauria, M.; Morine, M.J.; Moyseos, P.; Varma, V.; Nolen, G.T.; Knox, B.; Sloper, D.; Kaput, J.; et al. Systems view of adipogenesis via novel omics-driven and tissue-specific activity scoring of network functional modules. *Sci. Rep.* **2016**, *6*, 1–19.
24. Bernardo, M.E.; Zaffaroni, N.; Novara, F.; Cometa, A.M.; Avanzini, M.A.; Moretta, A.; Montagna, D.; Maccario, R.; Villa, R.; Daidone, M.G.; et al. Human bone marrow-derived mesenchymal stem cells do not undergo transformation after long-term in vitro culture and do not exhibit telomere maintenance mechanisms. *Cancer Res.* **2007**, *67*, 9142–9149.
25. Miura, M.; Miura, Y.; Padilla-Nash, H.M.; Molinolo, A.A.; Fu, B.; Patel, V.; Seo, B.-M.; Sonoyama, W.; Zheng, J.J.; Baker, C.C.; et al. Accumulated Chromosomal Instability in Murine Bone Marrow Mesenchymal Stem Cells Leads to Malignant Transformation. *Stem Cells* **2006**, *24*, 1095–1103.
26. Pinu, F.R.; Beale, D.J.; Paten, A.M.; Kouremenos, K.; Swarup, S.; Schirra, H.J.; Wishart, D. Systems Biology and Multi-Omics Integration: Viewpoints from the Metabolomics Research Community. *Metabolites* **2019**, *9*, 76.
27. Schwaiger, M.; Schoeny, H.; El Abiead, Y.; Hermann, G.; Rampler, E.; Koellensperger, G. Merging metabolomics and lipidomics into one analytical run. *Analyst* **2019**, *144*, 220–229.
28. Schwaiger, M.; Rampler, E.; Hermann, G.; Miklos, W.; Berger, W.; Koellensperger, G.; Schwaiger, M.; Rampler, E.; Hermann, G.; Miklos, W.; et al. Anion-Exchange Chromatography Coupled to High-Resolution Mass Spectrometry: A Powerful Tool for Merging Targeted and Non-targeted Metabolomics. *Anal. Chem.* **2017**, *89*, 7667–7674.
29. Rampler, E.; Schoeny, H.; Mitic, B.M.; El Abiead, Y.; Schwaiger, M.; Koellensperger, G. Simultaneous non-polar and polar lipid analysis by on-line combination of HILIC, RP and high resolution MS. *Analyst* **2018**, *143*, 1250–1258.
30. Rampler, E.; Criscuolo, A.; Zeller, M.; El Abiead, Y.; Schoeny, H.; Hermann, G.; Sokol, E.; Cook, K.; Peake, D.A.; Delanghe, B.; et al. A Novel Lipidomics Workflow for Improved Human Plasma Identification and Quantification Using RPLC-MSn Methods and Isotope Dilution Strategies. *Anal. Chem.* **2018**, *90*, 6494–6501.
31. Arisawa, K.; Ichi, I.; Yasukawa, Y.; Sone, Y.; Fujiwara, Y. Changes in the phospholipid fatty acid composition of the lipid droplet during the differentiation of 3T3-L1 adipocytes. *J. Biochem.* **2013**, *154*, 281–289.
32. Zhou, G.; Xia, J. OmicsNet: A web-based tool for creation and visual analysis of biological networks in

3D space. *Nucleic Acids Res.* **2018**, *46*, W514–W522.

33. Fei, W.; Du, X.; Yang, H. Seipin, adipogenesis and lipid droplets. *Trends Endocrinol. Metab.* **2011**, *22*, 204–210.
34. Martin, S.; Parton, R.G. Caveolin, cholesterol, and lipid bodies. *Semin. Cell Dev. Biol.* 2005, *16*, 163–174.
35. Prokesch, A.; Hackl, H.; Hakim-Weber, R.; Bornstein, S.; Trajanoski, Z. Novel Insights into Adipogenesis from Omics Data. *Curr. Med. Chem.* **2009**, *16*, 2952–2964.
36. Lu, Q.; Zhang, Y.; Elisseeff, J.H. Carnitine and acetylcarnitine modulate mesenchymal differentiation of adult stem cells. *J. Tissue Eng. Regen. Med.* **2015**, *9*, 1352–1362.
37. Tilg, H.; Moschen, A.R. Adipocytokines: mediators linking adipose tissue, inflammation and immunity. *Nat. Rev. Immunol.* **2006**, *6*, 772–783.
38. Ito, K.; Suda, T. Metabolic requirements for the maintenance of self-renewing stem cells. *Nat. Rev. Mol. Cell Biol.* **2014**, *15*, 243–56.
39. Yanes, O.; Clark, J.; Wong, D.M.; Patti, G.J.; Sanchez-ruiz, A.; Paul, H.; Trauger, S.A.; Desponts, C.; Ding, S.; Siuzdak, G. Metabolic oxidation regulates embryonic stem cell differentiation. *Nat. Chem. Biol.* **2010**, *6*, 411–417.
40. Shyh-Chang, N.; Daley, G.Q.; Cantley, L.C. Stem cell metabolism in tissue development and aging. *Development* **2013**, *140*, 2535–47.
41. Kha, H.T.; Basseri, B.; Shouhed, D.; Richardson, J.; Tetradis, S.; Hahn, T.J.; Parhami, F. Oxysterols regulate differentiation of mesenchymal stem cells: pro-bone and anti-fat. *J. Bone Miner. Res.* **2004**, *19*, 830–840.
42. Roberts, L.D.; Virtue, S.; Vidal-Puig, A.; Nicholls, A.W.; Griffin, J.L. Metabolic phenotyping of a model of adipocyte differentiation. *Physiol. Genomics* **2009**, *39*, 109–119.
43. Mingrone, G.; Greco, A. V.; Capristo, E.; Benedetti, G.; Giancaterini, A.; Gaetano, A. De; Gasbarrini, G. L-Carnitine Improves Glucose Disposal in Type 2 Diabetic Patients. *J. Am. Coll. Nutr.* **1999**, *18*, 77–82.
44. Lee, M.S.; Lee, H.J.; Lee, H.S.; Kim, Y. L-carnitine stimulates lipolysis via induction of the lipolytic gene expression and suppression of the adipogenic gene expression in 3T3-L1 adipocytes. *J. Med. Food* **2006**, *9*, 468–473.
45. Bergante, S.; Torretta, E.; Creo, P.; Sessarego, N.; Papini, N.; Piccoli, M.; Fania, C.; Cirillo, F.; Conforti, E.; Ghiroldi, A.; et al. Gangliosides as a potential new class of stem cell markers: The case of GD1a in human bone marrow mesenchymal stem cells. *J. Lipid Res.* **2014**, *55*, 549–560.
46. Moussavou, G.; Kwak, D.H.; Lim, M.U.; Kim, J.S.; Kim, S.U.; Chang, K.T.; Choo, Y.K. Role of gangliosides in the differentiation of human mesenchymal-derived stem cells into osteoblasts and neuronal cells. *BMB Rep.* **2013**, *46*, 527–532.
47. Nagafuku, M.; Sato, T.; Sato, S.; Shimizu, K.; Taira, T.; Inokuchi, J.I. Control of homeostatic and pathogenic balance in adipose tissue by ganglioside GM3. *Glycobiology* **2014**, *25*, 303–318.
48. Chong, J.; Soufan, O.; Li, C.; Caraus, I.; Li, S.; Bourque, G.; Wishart, D.S.; Xia, J. MetaboAnalyst 4.0: Towards more transparent and integrative metabolomics analysis. *Nucleic Acids Res.* **2018**, *46*, W486–W494.
49. AKHTAR, A. The Flaws and Human Harms of Animal Experimentation. *Cambridge Q. Healthc. Ethics* **2015**, *24*, 407–419.
50. Egger, D.; Schwedhelm, I.; Hansmann, J.; Kasper, C. Hypoxic Three-Dimensional Scaffold-Free Aggregate Cultivation of Mesenchymal Stem Cells in a Stirred Tank Reactor. *Bioengineering* **2017**, *4*, 47.
51. Vlassis, N.; Pacheco, M.P.; Sauter, T. Fast Reconstruction of Compact Context-Specific Metabolic

Network Models. *PLoS Comput. Biol.* **2014**, *10*.

52. Thiele, I.; Swainston, N.; Fleming, R.M.T.; Hoppe, A.; Sahoo, S.; Aurich, M.K.; Haraldsdottir, H.; Mo, M.L.; Rolfsson, O.; Stobbe, M.D.; et al. A community-driven global reconstruction of human metabolism. *Nat. Biotechnol.* **2013**, *31*, 419–425.